



HAL
open science

Innovative Optimization of Microgrid Configuration for Sustainable, Reliable and Economical Energy Using Homer Software

Habib Muhammad Usman, Nirma Kumari Sharma, Deepak Kumar Joshi, Aditya Kaushik, Sani Saminu

► **To cite this version:**

Habib Muhammad Usman, Nirma Kumari Sharma, Deepak Kumar Joshi, Aditya Kaushik, Sani Saminu. Innovative Optimization of Microgrid Configuration for Sustainable, Reliable and Economical Energy Using Homer Software. Research Square - Preprint, In press, 10.21203/rs.3.rs-4520716/v1 . hal-04622798

HAL Id: hal-04622798

<https://hal.science/hal-04622798>

Submitted on 24 Jun 2024

HAL is a multi-disciplinary open access archive for the deposit and dissemination of scientific research documents, whether they are published or not. The documents may come from teaching and research institutions in France or abroad, or from public or private research centers.

L'archive ouverte pluridisciplinaire **HAL**, est destinée au dépôt et à la diffusion de documents scientifiques de niveau recherche, publiés ou non, émanant des établissements d'enseignement et de recherche français ou étrangers, des laboratoires publics ou privés.

Innovative Optimization of Microgrid Configuration for Sustainable, Reliable and Economical Energy Using Homer Software

Habib Muhammad Usman

habibusman015@gmail.com

Mewar University

Nirma Kumari Sharma

Mewar University

Deepak Kumar Joshi

Mewar University

Aditya Kaushik

Mewar University

Sani Saminu

University of Ilorin

Research Article

Keywords: Renewable energy sources (RES), Levelized cost of energy (LCOE), HOMER software, Economical analysis, sensitivity analysis, optimization, Microgrid, Mewar University

Posted Date: June 18th, 2024

DOI: <https://doi.org/10.21203/rs.3.rs-4520716/v1>

License:  This work is licensed under a Creative Commons Attribution 4.0 International License.

[Read Full License](#)

Additional Declarations: No competing interests reported.

INNOVATIVE OPTIMIZATION OF MICROGRID CONFIGURATION FOR SUSTAINABLE, RELIABLE AND ECONOMICAL ENERGY USING HOMER SOFTWARE

Habib Muhammad Usman^{1*}, Nirma Kumari Sharma¹, Deepak Kumar Joshi¹, Aditya Kaushik¹, Sani Saminu²

¹*Department of Electrical Engineering, Mewar University, chittorgarh, Rajathan, India*

²*Department of Biomedical Engineering, University of Ilorin, Ilorin, Nigeria*

*Corresponding author email: habibusman015@gmail.com

*Corresponding author ORCID: <https://orcid.org/0009-0004-9584-7833>

Abstract

Mewar University grapples with exorbitant energy costs of approximately \$1kWh, unreliable power supply, and a significant reliance on diesel engines and the grid. This dependency not only escalates energy expenses but also contributes to greenhouse gas emissions, exacerbating climate change, global warming, and environmental pollution. To mitigate these issues, this study proposes an optimized microgrid design integrating PV solar panels, wind turbines, diesel generators, and grid connectivity, utilizing HOMER software for optimization. The software identified multiple configurations, with the optimal design meeting an energy demand of 20,077,351 kWh/year through a combination of solar PV (288,947,670 kWh annually), wind turbines (36,825,618 kWh annually), and minimal reliance on diesel generators. The system would purchase 3,827,194 kWh annually from the grid during low renewable output periods and sell 167,761,193 kWh annually during surplus production. This design achieves a levelized cost of energy (LCOE) of \$0.00146/kWh and a return on investment (ROI) of 10.1%, with total component expenditure of \$16,207,384, covering capital investments, operations and maintenance (O&M), and fuel costs. Solar photovoltaics contributes 83% of the annual production, with the remaining 17% from the grid and wind turbines, establishing the system as cost-effective and environmentally friendly due to its heavy reliance on renewable energy sources (RES). Comprehensive feasibility, technical, economic and sensitivity analyses confirm the viability of implementing this proposed system. Ultimately, the proposed microgrid design promises a sustainable, economical, and reliable energy solution for the University.

Keywords: Renewable energy sources (RES), Levelized cost of energy (LCOE), HOMER software, Economical analysis, sensitivity analysis, optimization, Microgrid, Mewar University.

1. Introduction

The rapid evolution of the global energy landscape has underscored the necessity for sustainable and resilient energy systems. Traditional centralized power grids face numerous challenges, including high transmission losses, vulnerability to outages, and the increasing pressure to integrate renewable energy sources. As a solution, microgrids have emerged as a promising technology to address these issues by offering localized, decentralized energy generation and distribution [1-2]. Microgrids can operate autonomously or in tandem with the main grid, enhancing reliability, efficiency, and sustainability [3-4]. The depletion of conventional energy reserves and growing environmental concerns have emerged as major worldwide challenges of this century [5-6]. Future energy demands are anticipated to be mostly met by hybrid renewable energy systems (RES) [7]. There are both financial and technological obstacles to extending the electrical grid to remote areas. By depending more on RES-based generation, these issues can be resolved [8]. This dependence has prompted research into and application of distributed power generation utilizing renewable energy sources. Renewable energy sources like solar and wind are good choices for producing electricity in remote areas because of their complementing qualities [9]. However, the sporadic and inconsistent character of these sources is one of their main drawbacks. When compared to single-source standalone systems, standalone hybrid renewable energy systems (RES) that combine solar and wind power are thought to be more dependable and feasible [10].

Only by addressing a number of critical issues will cost-effective generation be guaranteed: the best possible sizing of energy storage units (ESUs) and generators [11], power electronic converter interface control schemes, energy management policies [12], and the kind of ESUs and generators that are employed [13]. Hybrid wind-PV-storage systems can reliably power off-grid loads in some locations, such as hilltop load stations [14], small islands [15-16], broadcasting stations [17], satellite earth stations [18], eco-tourism sites [19], hotels [20], and similar locales [21]. The only common residential loads, tiny non-linear loads, and lighting loads are usually the only low power requirements at these sites [22]. In the context of typical Western Australian residential applications, Speidel and Braunl examined the viability and constraints of RES and ESU for both off-grid and grid-connected systems [23]. By using appropriate ESUs, the problem of power security for standalone RES applications can be reduced [24-25]. A number of parameters need to be taken into account when planning a site for the installation of RES-based generation, including load forecasting, conversion equipment sizing, and optimization approaches [26-27]. The use of hybrid wind-PV systems for electrifying off-grid communities [28], rural areas [29], islands [30], and minimizing the lifecycle cost of conversion components [31], is also covered in the literature.

The low efficiency of conversion equipment, sporadic and unpredictable meteorological data, and initial installation expenses are major obstacles to the broad implementation of renewable energy systems (RES) [32-33]. Two of the methods that have been published have shown to be extremely successful: making sure that spinning reserves are in place [34-36] and using the right storage unit services [37-40]. For isolated loads like islands, mountains, and off-grid areas, diesel generators are currently the main energy source [41]. However, because of the high cost of fuel handling and the difficulties associated with maintenance, diesel generators are neither practical nor economical for long-term use in these areas. They also have an adverse effect on the ecosystem. Luckily, there are usually plenty of locally accessible natural resources, such as solar and wind energy, in these remote areas. When considering the total cost of operation for diesel generators, the cost of generation can be considerably decreased by optimizing the sizing of these renewable energy systems [42]. Based on existing RES and including techno-economic analysis, an optimum PV/battery storage system (BS)/DG/Grid was designed in [43] for Diyala, Muqadiyah district, Iraq. [44] designed a PV/FC/Grid system to optimize LCOE and control grid interactions for an Indian university campus. [45] demonstrated cost-effective optimization based on RES availability by implementing a PV/WT/DG/Grid system at Malayer University in Iran. For Chintalayapalle village in Tadipatri, Andhra Pradesh, an ideal PV/WT/BS/Grid system with techno-economic and sensitivity assessments was suggested in [46]. [47] minimized NPC while adhering to reliability restrictions when designing a grid-connected PV power facility. [48] used heuristic and metaheuristic approaches to optimize a home energy system that included solar PV, fuel cells, and batteries. A worldwide comparison of stand-alone, grid-connected, and HRES PV systems was presented in [49], demonstrating how well-suited each is for various electrification requirements. For the King Saud University Campus in Riyadh, a hybrid solar, wind, and battery system linked to the grid was found to be the most beneficial option due to its cheap energy prices, dependability, low greenhouse gas emissions, and high penetration of renewable energy sources [50]. Microgrids integrate distributed energy resources such as storage devices and renewables to improve the resilience and dependability of the power grid. These locally controlled devices overcome the drawbacks of centralized grids by lowering air pollution, increasing energy efficiency, and maintaining independent operation during blackouts [51-54].

In their study, [64] assessed the financial and technical viability of various renewable energy technologies for telecommunications in India across twenty-one different locations. The study utilized the Levelized Cost of Energy (LCOE) to evaluate nine hybrid renewable power configurations. These configurations were analyzed based on power supply availability for varying durations (1hr, 2hrs, 4hrs, 8hrs, 12hrs, and 16hrs). Results indicated that the grid-connected solar PV power system had the lowest LCOE for 1hr of power unavailability, while a configuration combining grid-connected wind, solar PV, diesel generator, and battery achieved low LCOE with 4hrs of power unavailability. Similarly, Salisu et al. investigated a hybrid power system [65] aimed at reducing overall costs by integrating different renewable energy systems. Their optimization approach used multiple objective functions to select the optimal mix of resources that meet system load demand. Additionally, Essalaimeh et al. evaluated a

hybrid renewable energy system's performance in Jordan [66], using weather resources to model various load conditions with solar PV and wind technologies. Their study estimated a simple payback period using mathematical modeling to assess economic viability. Kabalci et al. designed a renewable energy power plant incorporating wind and solar PV systems [67]. Using the HOMER computational software, Li et al. performed a technical and economic assessment of a standalone microgrid system integrating solar PV, wind, and battery storage [68]. The microgrid configuration included a 5-kW solar PV system, a 2.5-kW wind turbine, 6.94 kWh unit batteries, and a 5-kW converter based on simulation results from the HOMER software. El Badawe et al. conducted a comparative analysis of renewable and non-renewable energy systems in Canada [69], using a telecommunications station as a case study energy consumer. The authors employed the HOMER computational software for the design, optimization, and simulation of proposed configurations. A configuration integrating a diesel generator proved cost-effective, reducing both the generator's running time and overall emissions and fuel consumption at the station. In [70], the authors proposed an integrated hybrid renewable energy (RE) power system incorporating an energy management system to enhance system efficiency and reduce energy costs. The effectiveness of the system was tested using the PSCAD platform. Daud et al. designed and analysed a hybrid energy system to supply electricity to a small family in Palestine [71]. The viability of the proposed system was modeled based on RE resource availability and load requirements. The authors developed a computer model to reduce the life-cycle cost and CO₂ emissions of the proposed hybrid renewable energy system for the Palestinian family.

Despite extensive research on hybrid renewable energy systems (HRES) in India and globally, there is limited literature specific to Rajasthan, even though the region has high solar irradiance and good wind speeds. Mewar University in Chittorgarh, Rajasthan, relies heavily on diesel generators and grid electricity, leading to high greenhouse gas emissions and costs. This study addresses these issues by designing an optimal HRES for the university and analysing the techno-economic feasibility of a grid-connected system. The proposed design is environmentally friendly and cost-effective, promoting sustainability. Additionally, it provides a roadmap for nearby villages in Chittorgarh to implement HRES. Using advanced simulation tools like HOMER (Hybrid Optimization of Multiple Energy Resources), the design, modeling, and optimization were successfully executed.

2. Method and Material

This section details the methodology employed to achieve the study's objectives. It outlines the energy audit process used to determine the load profile of the study area. Additionally, it describes the renewable energy resources, load profiles, cost inputs, and technical and economic parameters utilized for modelling and designing the proposed system. Specifically, it explains the use of the HOMER computational tool to size and design the proposed hybrid system and analyse the existing setup. Figure 1 illustrates the methodology framework used to meet the study's objectives.

2.1. Homer optimization software

The HOMER software is utilized to design, develop, and optimize the optimal Hybrid Renewable Energy System (HRES). This involves considering financial risks, environmental regulations, the availability of renewable energy resources, and specific renewable energy sources available in the chosen area. Effective design and planning of HRES require a daily load demand profile that incorporates seasonal variations, local meteorological data, site-specific conditions, and current power production capabilities of the system. Through simulation, optimization, and sensitivity analysis, HOMER software identifies the most cost-effective design of HRES. Parameters such as Net Present Cost (NPC), Levelized Cost of Energy (LCOE), and operation and maintenance (O&M) costs are comprehensively analysed using this approach. Additionally, HOMER conducts techno-economic analysis to determine the optimal HRES configuration. Sensitivity analysis evaluates the financial viability of the system under variable parameters [63]. In this study, the HOMER software is employed to design the best hybrid microgrid system based on the load profile of the selected location. The initial steps involve evaluating the area's load profile and collecting data on solar and wind potential.

Subsequently, various system components are selected to build the system, taking into account component sizes and cost considerations. Finally, optimization is performed to determine the cost-effectiveness of the HRES model. Figure 1 illustrates the methodology employed by HOMER software in this study.

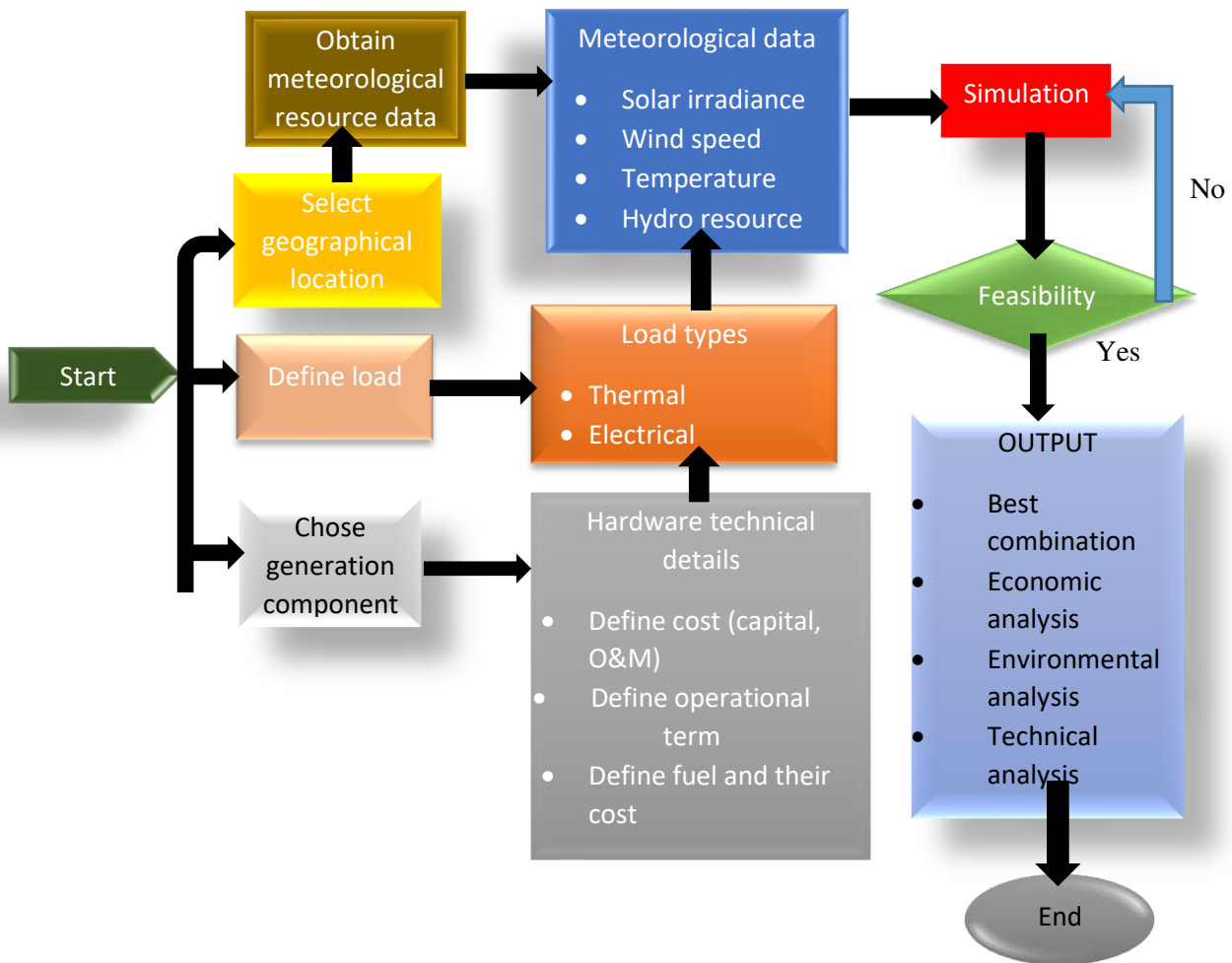


Figure 1: Homer optimisation procedure

2.2. Location of the study

The considered site for this study is Mewar University Gangrar, Chittorgarh, Rajasthan India with latitude and longitude of 25°1'56''N, 74°38'9''E and height of 40m from sea level. Figure 2 shows the map of the area of the study which was obtained from homer software.

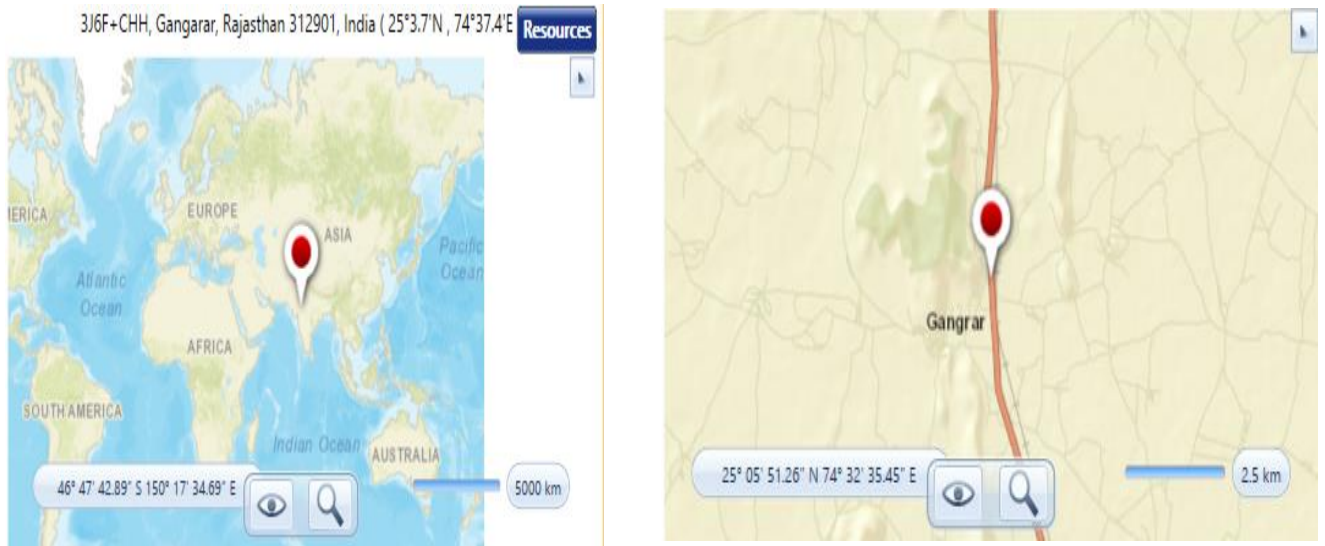


Figure 2: Research location

2.3. Load profile

To ascertain the load profile of the research region, the technique comprises an energy audit. The loads were documented for the following: Mewar Hospital; Bhamashah Hostel; Sanga Hostel; Kumbha Hostel; Pratap Hostel; Panna Dhai Hostel; Meera Hostel; Guest House; Staff Quarters (1 BHK); Staff Quarter; Administrative and Academic Block; Education Block; Engineering Block; and Annapurna Mess. Table 1 provides a summary of the yearly loads for these buildings, which were determined through the use of smart meters.

Table 1: Average monthly energy consumption

| Month | Energy consumed (kWh) |
|-----------|-----------------------|
| January | 60293 |
| February | 66850 |
| March | 66313 |
| April | 66589 |
| May | 44024 |
| June | 54980 |
| July | 63017 |
| August | 57103 |
| September | 63983 |
| October | 55121 |
| November | 33214 |
| December | 27790 |

Table 1 presents the average monthly energy consumption for the different university blocks. Between May (44,024 kWh) and June (54,980 kWh), when there are less academic activities at the university and energy usage is at its lowest, there is a notable drop. Comparably, because most classes, labs, seminars, practical sessions, and other university activities are not held over the holiday season, November (33,214 kWh) and December (2,7790 kWh) exhibit lower energy usage. With reduced usage during the holidays and higher demand during times of regular university activities, this chart illustrates how the academic calendar affects energy consumption.

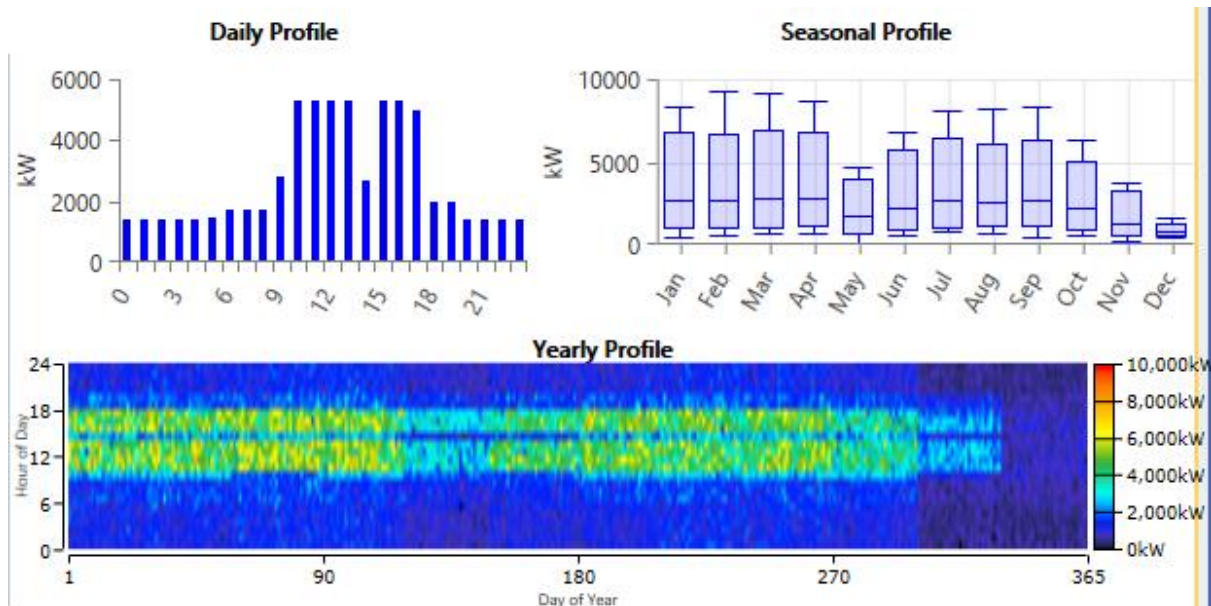


Figure 3: Daily, seasonal and yearly load profile

The profiles of daily, seasonal, and annual energy use are shown in Figure 3. According to the daily profile, demand peaks between 9 AM and 5 PM, and then significantly declines between 1 PM and 2 PM because of a break during which all labs, classes, and other activities are suspended. Monthly consumption peaks in January, February, March, April, July, August, September, and October, according to the seasonal profile. The annual profile shows the peak demand, indicated in yellow, which is normally between 9 AM and 5 PM, with a dip between 1 PM and 2 PM. The peak demand falls between 6000 and 8000 kW. Figure 3 illustrates how energy use drops to the 2000–4000 kW range (indicated in blue) during non-working hours.

2.4. Resources Assessment

Solar photovoltaic (PV) and wind energy are included in this study as renewable energy sources (RES). As a result, measurements of sun radiation and wind speed were made both annually and monthly. The HOMER software measures wind speed and solar irradiance by using data from solar energy and NASA surface meteorology. To ascertain the ideal Grid-Integrated Hybrid Microgrid System (GIHMGS) scaling, a number of modeling factors, including technical, economic, and social ones, were taken into account.

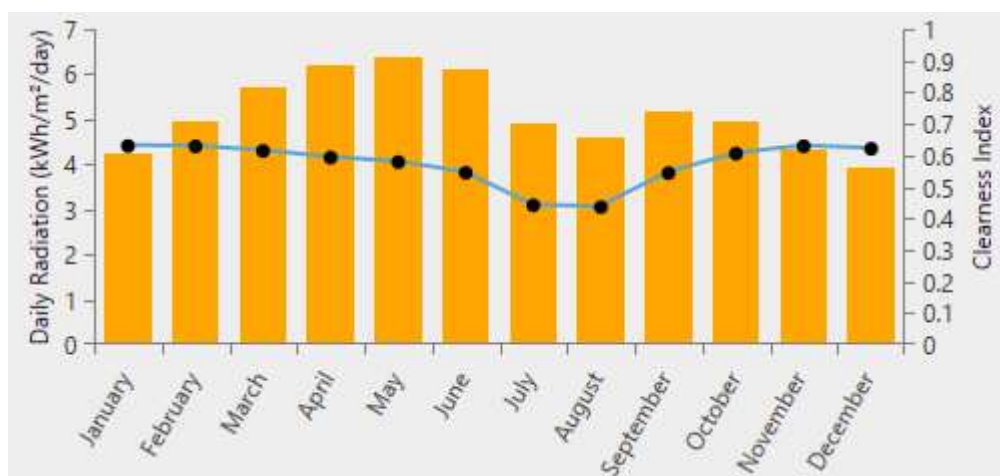


Figure 4: Monthly average global horizontal irradiance

Table2: Monthly average global horizontal irradiance

| Month | Clearness index | Daily radiation (kWh/m ² /day) |
|-----------|-----------------|---|
| January | 0.629 | 4.220 |
| February | 0.628 | 4.930 |
| March | 0.613 | 5.690 |
| April | 0.592 | 6.180 |
| May | 0.578 | 6.390 |
| June | 0.544 | 6.110 |
| July | 0.441 | 4.890 |
| August | 0.435 | 4.600 |
| September | 0.543 | 5.190 |
| October | 0.604 | 4.940 |
| November | 0.628 | 4.340 |
| December | 0.620 | 3.930 |

Using information from NASA, the study evaluates solar radiation for Mewar University in Chittorgarh, Rajasthan. The monthly average globally horizontal irradiance, together with the daily radiation in kWh/m²/day and the clearness index, are shown in Table 2 and Figure 4. The data reflects seasonal fluctuations in solar energy availability in the area. Solar radiation varies throughout the year, with greater concentrations during the summer months (April to June) and lower values in the winter months (November to January).



Figure 5: Monthly average wind speed data

Table 3: Monthly average wind speed data

| Month | Average wind speed (m/s) |
|-----------|--------------------------|
| January | 3.130 |
| February | 3.580 |
| March | 3.200 |
| April | 4.120 |
| May | 4.850 |
| June | 4.970 |
| July | 4.240 |
| August | 3.540 |
| September | 3.510 |
| October | 2.900 |
| November | 2.930 |

| | |
|----------|-------|
| December | 3.040 |
|----------|-------|

Using NASA data, the study assesses the potential for wind energy at Mewar University in Chittorgarh, Rajasthan. The monthly average wind speed data are shown in Table 3 and Figure 5, which show seasonal fluctuations. The summer months of April through July see higher wind speeds, reaching their highest point in June at 4.97 m/s. The winter months of October through February see lower wind speeds, reaching their lowest point in October at 2.9 m/s with an average speed of 3.67m/s.

2.5. Components selection

Table 4: components used in the proposed design

| Components | Manufacturers | Quantity | Rating (kW) | Capital (\$) | Replacement (\$) | O & M (\$) |
|------------------|-----------------------------------|----------|-------------|--------------|------------------|------------|
| PV panel | Generic flat plate PV | 148 | 1000 | 4,300,420 | 3,133,311 | 3,670 |
| Wind turbine | Generic 1MW | 26 | 1000 | 2,001,600 | 1,507,390 | 5,168 |
| Diesel generator | Generic 1MW fixed capacity Genset | 1 | 1000 | 35000 | 35000 | 200 |
| Converter | Generic System converter | 14 | 41,880 | 837,600 | 837,600 | 500 |
| Grid | Grid | 1 | 999,999 | 0.00 | 0.00 | 3,509,425 |

Using HOMER software and cost analysis, a variety of components were chosen for the microgrid architecture used in this study. A diesel generator, converters, PV panels, wind turbines, and a grid connection are among the parts listed in Table 4. With a total capital cost of \$4,300,420 and yearly operating and maintenance (O&M) costs of \$3,670 per panel, the PV panels are made up of 148 basic flat plate PV panels with a 1000 kW rating each. 26 typical 1 MW turbines, each costing \$2,001,600, are included in the wind turbines. Each turbine has yearly O&M expenses of \$5,168. A single 1 MW diesel generator has an annual O&M cost of \$200 and a capital cost of \$35,000. The total capital cost of fourteen generic system converters, each rated at 41,880 kW, is \$837,600. Each converter has an annual O&M cost of \$500. At a capital cost of \$999,999 and an annual operating and maintenance cost of \$3,509,425 the microgrid is also connected to the grid. These elements were chosen to maximize the microgrid system's performance for the research region based on their technical attributes and financial viability.

2.6. Design and modelling of Microgrid

The grid-connected microgrid design was developed using the HOMER software, as depicted in Figure 6. The components were meticulously modeled, designed, optimized, and sized to ensure efficient integration and operation within the existing grid infrastructure.

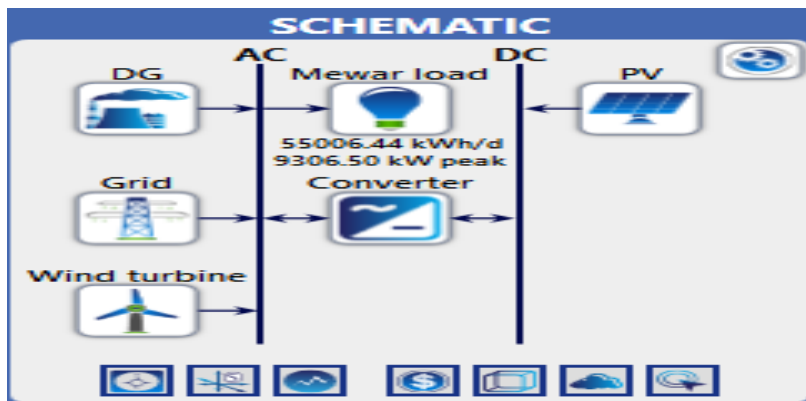


Figure 6: Grid connected microgrid design

2.6.1. PV system modeling

One of India's main renewable energy sources for electricity generation is solar energy, especially in rural areas with limited access to the utility grid [56]. A solar PV module's power output is directly correlated with the site's solar radiation (SR) levels. Equation (1), which is dependent on the observed solar radiation and atmospheric temperature, can be used to determine the hourly performance of solar photovoltaic panels [57].

$$P_{PV} = Y_{PV} f_{PV} \left(\frac{G_T}{G_{T,STC}} \right) [1 + \alpha_p (T_C - T_{C,STC})] \quad (1)$$

Where Y_{PV} is the solar PV's relative capacity in KW, f_{PV} is the derating factor of the solar PV in %, G_T is the SR on the solar PV in the present period in kWh/m²/d, $G_{T,STC}$ is the SR at STC Kw/m², α_p is the power's temperature coefficient-0.5%/°C, T_C is the temperature of PV cell's in a given period %/°C and $T_{C,STC}$ is the solar PV's temperature at STC of 25°C.

The annual maintenance costs (O&M) of a solar PV array can be as little as \$10 per kW, depending on labor costs and shipping expenses from the production location. The primary drawback of the solar PV system is that it is completely worthless and would require as much money for replacement as it did for installation. When the ground reflectance is set at 30% and the solar panel derating factor is adjusted to 0.96 (usually between 0.7 and 0.98), the system efficiency increases [58].

2.6.2. Wind Turbine Modelling

The wind turbine in this study runs at maximum power efficiency with an average cut-in speed of 3.67 m/s. Every time step, a wind turbine (WT) system assesses how much power it generates. Equation (2) is used to compute the turbine's wind speed [59].

$$U_{hub} = U_{anem} \times \frac{\ln\left(\frac{Z_{hub}}{Z_0}\right)}{\ln\left(\frac{Z_{anem}}{Z_0}\right)} \quad (2)$$

U_{hub} is the wind speed in meters per second at the hub height (HH), U_{anem} = wind speed at the anemometer's height in meters per second; ln = natural logarithm; Z_{hub} = turbine's height in meters; Z_{anem} = anemometer's height in meters Z_0 = roughness length of the surface in meters, ln = Natural logarithm.

Equation (2) is used to calculate the wind turbine's (WT) output power under typical operating conditions [59].

$$P_{WTG} = \left(\frac{\rho}{\rho_0} \right) \times P_{WTG,STP} \quad (3)$$

Where the wind turbine's output power is expressed in kW as P_{WTG} ; the actual air density is represented as ρ and expressed in kg/m³; ρ_0 is the air density at standard pressure and temperature (1.225 kg/m³); and $P_{WTG,STP}$ is the wind turbine's output power at standard pressure and temperature measured in kW [57]

$$P_{WT} = \left[V^3 \left(\frac{P_r}{V_r^3 - V_{cutin}^3} \right) - \left(\frac{V_{cutin}^3}{V_r^3 - V_{cutin}^3} \right) \times P_r \right] \quad (4)$$

Where P_{WT} is the turbine output power, P_r is the rated power of the WT, V_r is the rated speed of WT, V_{cutin} and V_{cutout} are cut-in and cut-out speed of the wind

2.6.3. Diesel generator modelling

A diesel generator (DG) is utilized as a backup to deliver power and meet customer demand during peak periods when the amount of power generated by renewable energy sources (RES) drops. For the Grid-Integrated Hybrid Microgrid System (GIHMGS) architecture, an auto-sized Kohler DG is chosen using the HOMER software. This Kohler DG automatically adapts to fulfill load requirements in any situation [60]. The DG operates as a single power system in the event that the total amount of electricity generated by storage cells and non-conventional energy sources is insufficient to meet load needs. Equation (5) determines the power output at each time step by taking the gas volume of the diesel generator [57].

$$F_{cons} = a. P_{DG} + b. P_{DG,r} \quad (5)$$

Where F_{cons} _Fuel consumption (L/hr), P_{DG} _ power generated by DG (kW), $P_{DG,r}$ _Rated power of the DG generated on hourly basis (t), a and b are the constant measured in (L/kW)

2.6.4. Converter

When designing a Grid-Integrated Hybrid Microgrid System (GIHMGS), a generic converter can effectively convert the entire power produced by renewable energy sources (RES) [61]. The converter's size, capacity, and design specifications all have a big impact on the price. With a 15-year lifespan and relative capacities and efficiencies of 100% and 95%, respectively, equation (6) calculates the lifetime of the inverter and rectifier inputs [59]. To supply the AC load in this study, however, a single inverter was used in the design to convert the DC power produced by the PV panels into AC power.

$$\eta_{con} = \frac{P_{out}}{P_{in}} \quad (6)$$

Where η_{con} = Converter efficiency, P_{out} = Output power of the converter, P_{in} = Input power of the converter.

2.6.5. Grid

In this study, Electricity Distribution Company Limited (EDCL) delivered energy for \$0.1 per kWh and excess electricity generated by the Grid-Integrated Hybrid Microgrid System (GIHMGS) is sold back to the utility grid at a \$0.01 per kWh feed-in tariff rate. The total annual energy charge is determined using equation (7).

$$C_{grid,energy} = \sum_{n=l}^{rates} \sum_{n=m}^{12} E_{gridpurchases,l,m} \times C_{power,l} - \sum_{n=i}^{rates} \sum_{n=m}^{12} E_{gridsales,l,m} \times C_{saleback,l} \quad (7)$$

Where $C_{grid,energy}$ _ The total annual energy charge, $E_{gridpurchases,l,m}$ _ The energy purchased amount from the grid in m month during the time that rate l applies (kWh), $C_{power,l}$ _ The grid price for rate l (\$/kWh), $E_{gridsales,l,m}$ _ The amount of energy sold to the grid in month m during the time that l rate applies (kWh), $C_{saleback,l}$ _ The sell back rate for rate l (\$/kWh).

2.7. Techno-Economic analysis

The system's overall cost includes the price of each ideal component. The Levelized Cost of Energy (LCOE) and Net Present Cost (NPC) are computed using the annualized cost of the system. The NPC and LCOE have a major impact on the design of the proposed system. The NPC methodology is compatible with different hybrid renewable energy system (HRES) configurations that are built in the course of optimization [62].

2.7.1. Levelized Cost of Energy (LCOE): The cost per unit of energy produced is the LCOE for the HRES. Stated otherwise, it is the ratio, as determined by Equation (8) [57], of the system's yearly cost to the total amount of energy units produced by the HRES:

$$LCOE = \frac{\text{Total annualized cost (\$)}}{\text{Total energy generated (kWh)}} \quad (8)$$

2.7.2. Capital Recovery Factor (CRF): Equation (9) is used to compute it [57].

$$CRF(i, n) = \left[\frac{i(1+i)^n}{(1+i)^n - 1} \right] \quad (9)$$

Where "i" stands for the yearly interest rate (%) and "n" for the number of years. A reduction in interest rates could result in a lower CRF, which would raise the NPC.

2.7.3. Net Present Cost (NPC): It is represented using "the total annualized cost and the LCOE of the system." The NPC is given by the following Equation (10) [57]:

$$D_{NPC} = \frac{D_{total,annual}}{CRF(i, L_{proj})} \quad (10)$$

Where $D_{total,annual}$ – Total annualized cost per year (\$/yr), i – Annual interest rate (%) or discount rate, L_{proj} – Life span of the project in year, $CRF(i, L_{proj})$ – Capital recovery factor with i expressed as percentage of the interest rate.

2.7.4. A renewable fraction, or RF fraction: is "the fraction of power produced from renewable sources and transferred to the system." Calculated with Equation (11) [57], it is dimensionless and denoted as f_{ren} .

$$f_{ren} = 1 - \frac{E_{non,ren} + H_{non,ren}}{E_{served} + H_{served}} \quad (11)$$

Where $E_{non,ren}$ – Non-renewable electrical energy production (kWh/yr), $H_{non,ren}$ – Non-renewable thermal energy production (kWh/yr), E_{served} – Total electrical load served (kWh/yr) and H_{served} – Total thermal load served (kWh/yr)

2.7 Technical constraints

Several technical limitations were used in this study to analyze the hybrid renewable energy system (HRES). Among them is a minimum renewable portion of 70%, which guarantees that the energy generated originates from renewable sources to the extent of at least 70%. 10% of the yearly peak load and 20% of the present time step demands must be met by the load. The maximum outputs for solar and wind electricity are regulated at 85% and 25% of their respective potential outputs. With an annual purchasing capacity of 3,827,194 kW, the grid's real-time capacity is set at 999,999 kW. For a 100-kilometer stretch, the grid capital cost is set at \$10,000 per kilometer. Furthermore, grid rate parameters are produced at random, producing 8,760 lines of data including sell-back and power prices.

3. Result and Discussion

Homer provides numerous optimization results in order of their optimality. However the most optimal results are suggested by the software. It selects the optimal results base on several factor such as initial cost, operating cost and maintenance cost, sensitivity, return on investment, levelized cost of energy (LCOE), annualised cost, net present cost, sensitivity to fuel prices, renewable fluctuation, degradation, Grid energy prices and emission such as, Carbon Dioxide, Carbon Monoxide, Unburned Hydrocarbons, Particulate Matter, Sulfur Dioxide, Nitrogen Oxides and flexibility etc. the most optimal result is proposed by the software and compared with the base case. Figure 7 shows the base case and the optimal result.

| Component | Base Case Value | Proposed Design Value |
|----------------|-----------------|-----------------------|
| PV (kW) | 55,008 | 164,036 |
| G3 | | 55,008 |
| 1MWGen (kW) | 1,000 | 1,000 |
| Grid (kW) | 999,999 | 999,999 |
| Converter (kW) | 41,630 | 41,630 |

Figure 7: optimization result of the base case and proposed design

As shown in the Figure 7, in the base case, all the energy demands are met with Wind turbine energy generator and grid, while in the proposed design, the demands are met by solar PV, wind turbine, diesel generator and grid.

3.1. Base case result analysis

Table 5: Wind turbine rating and energy production

| Quantity | Value | Unit |
|----------------------|------------|--------|
| Total Rated Capacity | 165,024 | kW |
| Mean Output | 4,204 | kW |
| Capacity Factor | 2.55 | % |
| Total Production | 67,056,840 | kWh/yr |
| Minimum Output | 0 | kW |
| Maximum Output | 161,020 | kW |
| Hours of Operation | 4,327 | hrs/yr |
| AC Primary Load | 20,077,351 | kWh/yr |
| DC Primary Load | 0 | kWh/yr |

Table 6: Base case- summary of energy purchased, sold, charges and profit

| Month | Energy Purchased (kWh) | Energy Sold (kWh) | Peak Demand (kWh) | Energy Charges (\$) | Energy Sold (\$) | Net Energy profit (\$) |
|-----------|------------------------|-------------------|-------------------|---------------------|------------------|------------------------|
| January | 525927 | 2625406 | 3129 | 52593 | 26254 | -26,339 |
| February | 404571 | 2880563 | 3137 | 40457 | 28807 | -11,650 |
| March | 477064 | 2730671 | 3144 | 47706 | 27307 | -20,399 |
| April | 325277 | 4289800 | 2971 | 32528 | 42898 | 10,370 |
| May | 179350 | 7148779 | 1900 | 17935 | 71488 | 53,553 |
| June | 221967 | 6981243 | 3032 | 22197 | 69812 | 47,615 |
| July | 292122 | 4634573 | 3249 | 29212 | 46346 | 17,134 |
| August | 397375 | 3242951 | 3055 | 39738 | 32430 | -6,931 |
| September | 393606 | 2996201 | 3606 | 39361 | 29962 | -9,399 |

| | | | | | | |
|----------|---------|----------|------|--------|--------|---------|
| October | 471437 | 2822997 | 2739 | 47144 | 28230 | -18,914 |
| November | 256230 | 3075393 | 2705 | 25623 | 30754 | 5,131 |
| December | 219315 | 3550897 | 1173 | 21932 | 35509 | 13,577 |
| Annual | 4164246 | 46979478 | 3606 | 416423 | 469795 | 53,748 |

Table 7: Base case-Economic summary

| Components | Capital(\$) | Replacement (\$) | O & M (\$) | Fuel (\$) | Total (\$) |
|--------------|-------------|------------------|------------|-----------|------------|
| Wind Turbine | 6,491,800 | 3,511,168 | 11,000 | 0.0 | 10,013,968 |
| Grid | 0.0 | 0.0 | 3,509,425 | 0.0 | 3,509,425 |
| | 6,491,800 | 3,511,168 | 3,520,425 | 0.0 | 13,523393 |

Table 8: Base case-Cost analysis

| Metric | Value |
|--------------------------|-------------|
| Present worth (\$) | \$13,523393 |
| Annual worth (\$/yr) | \$73,026 |
| Return on investment (%) | 0.54 |
| Levelized Cost of Energy | 0.0413 |

As shown in the Table 5, wind energy system reveals a low capacity factor of 2.55%, significantly below industry standards, indicating underperformance potentially due to poor wind conditions or inefficiencies. Despite generating 67,056,840kWh annually and having a total rated capacity of 165,024 kW, the system's economic viability is challenged by high costs and modest profits. The annual net profit stands at \$53,748 as highlighted in Table 6, but with an ROI of only 0.54%, the financial returns are minimal as depicted in Table 8. Monthly financial outcomes vary widely, suggesting a need for better energy management and cost reduction strategies as Table 7 shows. The average cost of producing one kWh of electricity is \$0.0413, which is known as the levelized cost of energy (LCOE) as depicted in Table 8. Although this LCOE is competitive when compared to conventional energy sources, the system's total economic appeal is reduced by its high prices and low capacity factor.

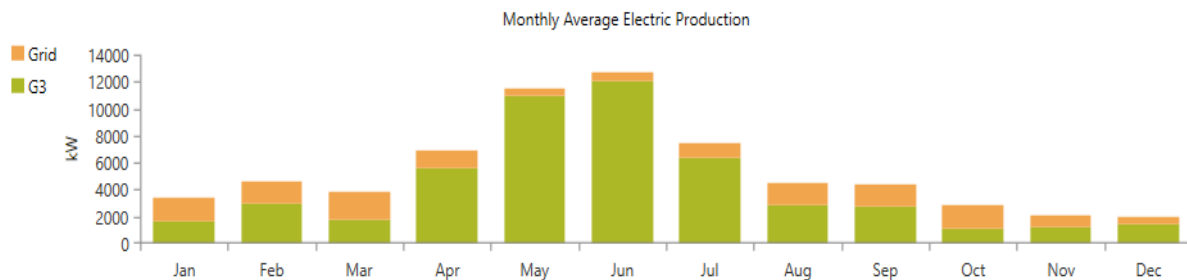


Figure 4: Base case- Annual energy production from wind and Grid

The base case scenario is depicted in Figure 8, which shows the annual energy production from wind and grid sources. The wind energy system generates a significant 36,825,618 kWh annually, indicating its primary role in meeting energy needs. However, because of a low capacity factor of 2.55%, additional energy is needed from the grid, totalling 4,164,246 kWh annually. This figure shows that although the majority of the energy is generated by the wind turbines, grid energy acts as a vital backup to ensure consistent supply.

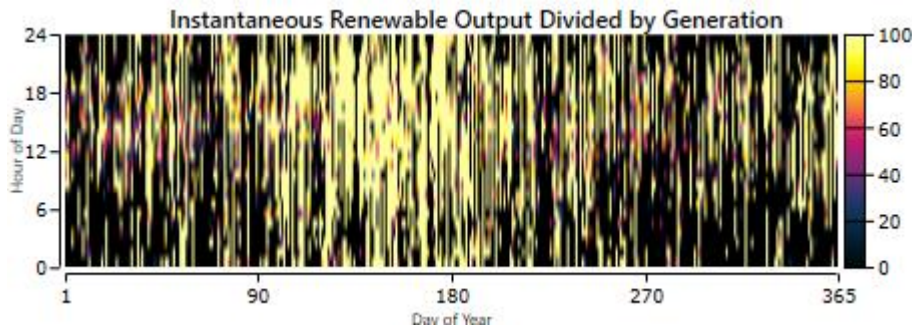


Figure 9: Base case- instantaneous wind power generated divided by total generation

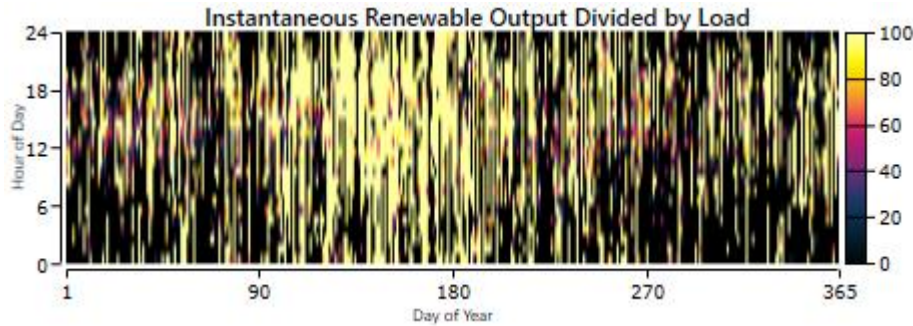


Figure 10: Base case- instantaneous wind output divided by the load

The instantaneous wind power output is shown in Figures 9 and 10 in two different contexts: as a percentage of the overall generation and as a percentage of the load. The power output levels are shown by several color on the graphs: brown denotes power output between 60 and 100 kW, pink 40-60 kW, blue 20-40 kW, and dark areas denote no generation. These graphs illustrate the erratic nature of wind energy production by displaying periods of high, moderate, and no generation. The dark portions of the graphs indicate the need for energy purchases from the grid to meet demand when wind speeds decrease and generation stops. This fluctuation highlights how wind energy is sporadic and how a reliable energy source requires grid backup.

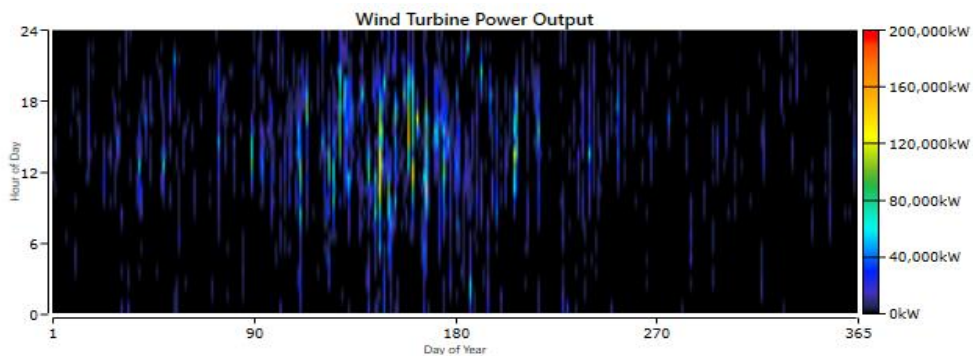


Figure 11: Base case- wind turbine power output

The wind turbines' immediate wind power generation is shown in Figure 11. The power output levels on the graph are represented by the colours black and blue, which range from 0 to 40,000 kW. These colours' non-uniform distribution, which reflects different wind speeds, shows variations in wind turbine generation. This illustration emphasizes the sporadic character of wind energy by demonstrating how variations in wind speed can cause power generation to fluctuate dramatically over brief intervals of time.

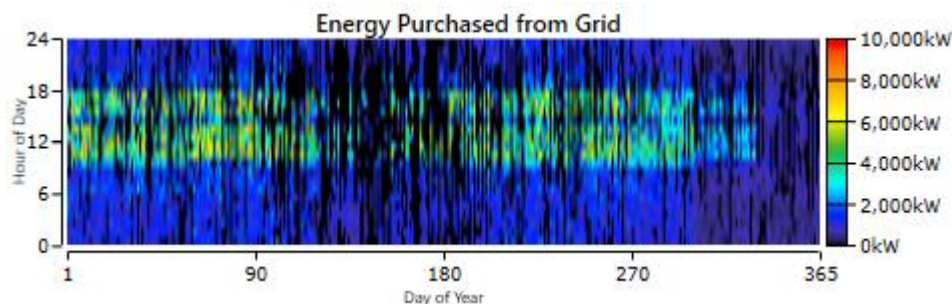


Figure 12: Base case- energy purchased from the grid

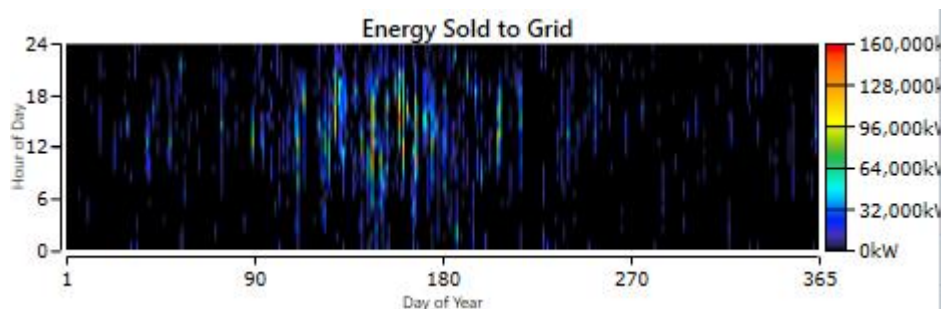


Figure 13: Base case- energy sold to the grid

The electricity bought from the grid over a 24-hour period is shown in Figure 12. The graph illustrates higher energy demand between 9 am and 5 pm as a result of university activities including lectures, practical, and administration. Grid purchases between 4000 and 6000 kW are shown by the brown colour. The colour changes to dark blue during off-peak hours (6 p.m. to 8 a.m.), signifying smaller grid purchases between 0 and 2000 kW. The energy sold to the grid is shown in Figure 13. With sporadic blue patches showing grid sales, the graph is primarily dark, signifying no grid sales. When surplus energy is produced and sold to the grid to satisfy demand, these blue patches appear. On the other hand, as Figure 12 illustrates, energy is imported from the grid when energy production falls short of demand. The dynamic relationship between energy production and consumption in a university context is illustrated by these data. They show how the system can use grid interactions to balance supply and demand for energy, resulting in a steady and dependable supply of electricity during peak and off-peak hours.

3.2. Proposed Design Result and Discussion

Table 9: Summary of solar PV, wind turbine and diesel generator rating and capacity

| Quantity | PV | Wind turbine | Unit |
|--------------------|-------------|--------------|--------|
| Rated Capacity | 165,021 | 165,024 | kW |
| Mean Output | 32,985 | 4,204 | kW |
| Mean Output | 791,637 | - | kWh/d |
| Capacity Factor | 45.0 | 2.55 | % |
| Total Production | 288,947,670 | 16,825,618 | kWh/yr |
| Minimum Output | 0 | 0 | kW |
| Maximum Output | 177,973 | 161,020 | kW |
| Hours of Operation | 4,398 | 4,327 | hrs/yr |
| AC Primary Load | 20,077,351 | 20,077,351 | kWh/yr |
| DC Primary Load | 0 | 0 | kWh/yr |

Table 10: Optimal case- summary of energy purchased, sold, charges and profit

| Month | Energy Purchased (kWh) | Energy Sold (kWh) | Peak Demand (kWh) | Energy Charges (\$) | Energy Sold (\$) | Net Energy profit (\$) |
|-----------|------------------------|-------------------|-------------------|---------------------|------------------|------------------------|
| January | 490572 | 11370903 | 3129 | 49057 | 113709 | 64,652 |
| February | 369341 | 11792373 | 3137 | 36934 | 117924 | 80,990 |
| March | 446509 | 12189770 | 3144 | 44651 | 121898 | 77,247 |
| April | 295564 | 15420409 | 2730 | 29556 | 154204 | 124,648 |
| May | 163224 | 21025727 | 1900 | 16322 | 210257 | 193,935 |
| June | 200899 | 20851229 | 2884 | 20090 | 208512 | 188,422 |
| July | 254856 | 15449317 | 2381 | 25486 | 154493 | 129,007 |
| August | 362233 | 12118163 | 2672 | 36223 | 121182 | 84,959 |
| September | 347097 | 11841843 | 2637 | 34710 | 118418 | 83,708 |
| October | 441685 | 11924716 | 2739 | 44169 | 119247 | 75,078 |
| November | 243438 | 11597432 | 2416 | 24344 | 115974 | 91630 |
| December | 211770 | 12179307 | 1150 | 21177 | 121793 | 100,616 |
| Annual | 3827194 | 167761193 | 3144 | 382719 | 1677612 | 1,294,892 |

Table 11: Proposed design -Cost of the components

| Component | Capital (\$) | Replacement (\$) | O & M (\$) | Fuel (\$) | Total (\$) |
|-----------------------|--------------|------------------|------------|-----------|------------|
| Wind turbine | 2,001,600 | 1,507,390 | 5,168 | 0 | 3,514,158 |
| Generic flat plate PV | 4,300,420 | 3,133,311 | 3,670 | 0 | 7,437,401 |
| Diesel Generator | 35000 | 35000 | 200 | 500 | 70,700 |
| Grid | 0.00 | 0.00 | 3,509,425 | 0.0 | 3,509,425 |
| System Converter | 837,600 | 837,600 | 500 | 0 | 1,675,700 |
| | 7,174,620 | 5,513,301 | 3,518,963 | 500 | 16,207,384 |

Table 12: Proposed design-Economic analysis

| Metric | Value |
|-------------------------------|---------------|
| Present worth (\$) | \$16,207,384 |
| Annual worth (\$/yr) | \$1,782,812 |
| Return on investment (%) | 10.1 |
| Levelized Cost of energy LCOE | 0.00146\$/kWh |

With a capacity factor of 45.0%, the solar PV system in this proposed design generates 288,947,670 kWh annually with a mean output of 32,985 kW. This is a significant increase in energy production over the base case and shows better utilization of the system's capacity. The wind turbine system, rated at 165,024 kW with a capacity factor of 2.55%, generates 36,825,618 kWh annually with a mean output of 4,204 kW as depicted in Table 9. Despite the low capacity factor, improvements in operational efficiency have raised both mean output and total energy production. The proposed design has a \$1,294,892 yearly net energy profit, making it substantially more profitable financially as itemized in Table 10. Energy management techniques that balance energy sales and purchases are the driving force behind this progress. When production is higher than demand, especially during peak university events, the system sells the excess energy back to the grid. It also purchases energy during low production periods, such as non-working hours. The steady and continuously positive monthly profitability is indicative of a more effective utilization of renewable energy resources. The levelized cost of energy (LCOE) of \$0.00146/kWh and the return on investment (ROI) of 10.1%, respectively, are

improvements over the previous scenario according to the proposed design's economic analysis as shown in Table 12. The low LCOE shows the system's cost-effectiveness over its operational life, while the ROI shows a favourable financial return on the initial investment. These measurements demonstrate how much more competitive and economically viable the system is when compared to conventional energy sources. The proposed design entails component expenditures of \$16,207,384, which comprise capital investments, replacements, operations & maintenance (O&M) costs, and fuel costs as Table 11 depicts. By using parts like the system converter and diesel generator, this investment guarantees a backup energy supply and promotes dependable energy output.

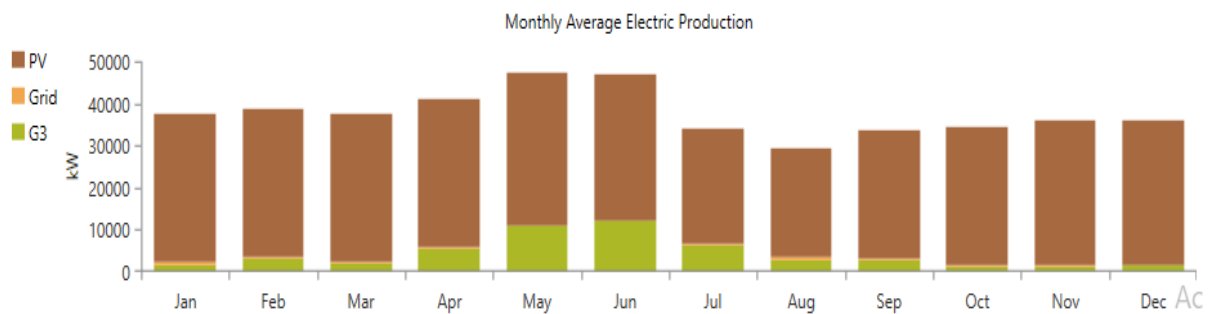


Figure 14: Optimal case- energy production from solar PV, wind and grid throughout the year

The distribution of energy production in the proposed design is shown in Figure 14. According to the data, 83% of the annual energy production is attributed to solar photovoltaics. The grid and wind turbines provide the remaining 17%. While wind turbines and grid electricity give crucial support to meet the overall energy demand, solar PV's noteworthy contribution emphasizes its leading role in the energy mix.

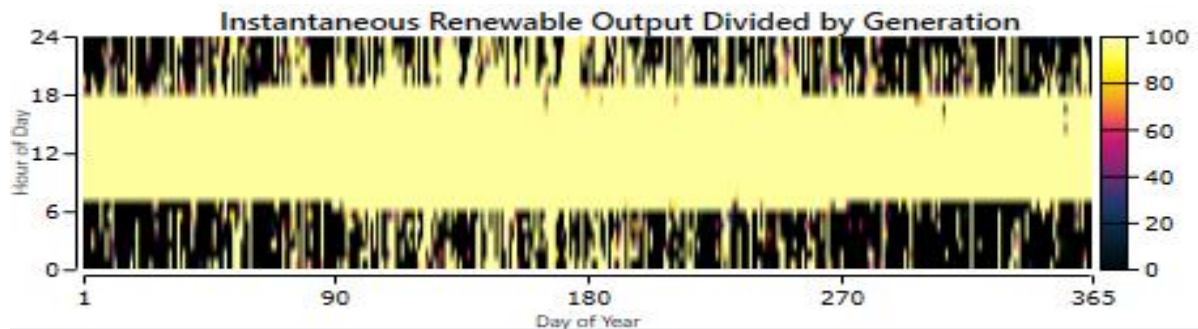


Figure 15: Optimal case- instantaneous solar and wind output divided by generation

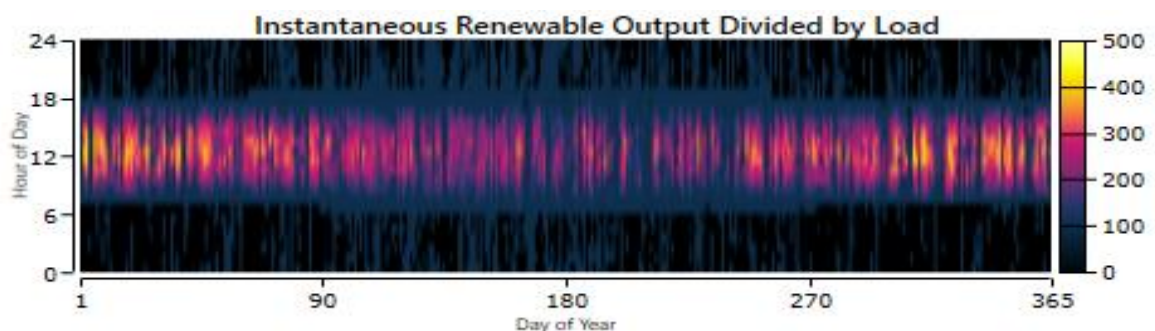


Figure 16: Optimal case- instantaneous solar and wind output divided by load

The instantaneous renewable energy output is shown in Figures 15 and 16 in two different contexts: split by total generation and divided by load, respectively. The graph's predominant brown colour between 7 am and 6 pm indicates that the renewable energy systems are producing 80–100 kW. In Gangrar, Chittorgarh, Rajasthan, this time of day corresponds to high solar intensity, which causes the solar PV system to produce a significant amount of energy—often more than needed during the day. In this period, the wind turbine generates extra electricity to supplement the photovoltaic system. The lack of sunshine causes a shift in energy production from 6 p.m. to 6 a.m. The graph's blend of pink and black hues during these hours indicates that the wind turbine is the only source of renewable energy generated, with outputs varying from negligible to moderate. As a result, more energy must be drawn from the grid to satisfy the demand. This pattern is further demonstrated in Figure 16, which shows the renewable output in relation to the load. The colour is dark pink throughout the day, which indicates a greater renewable output (between 100 and 200 kW) that either fully matches or surpasses the load. However, the graph darkens at night, showing a reduced output of renewable energy and a growing reliance on grid energy to satisfy the demand.

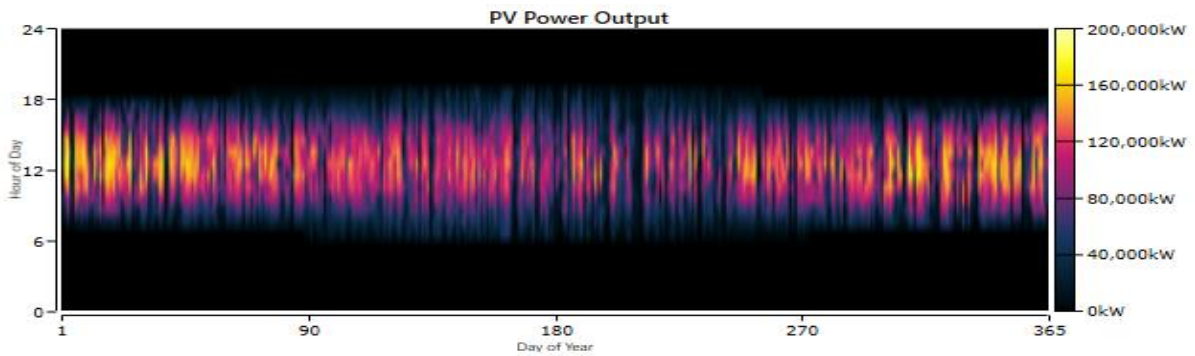


Figure 17: optimal design PV power output

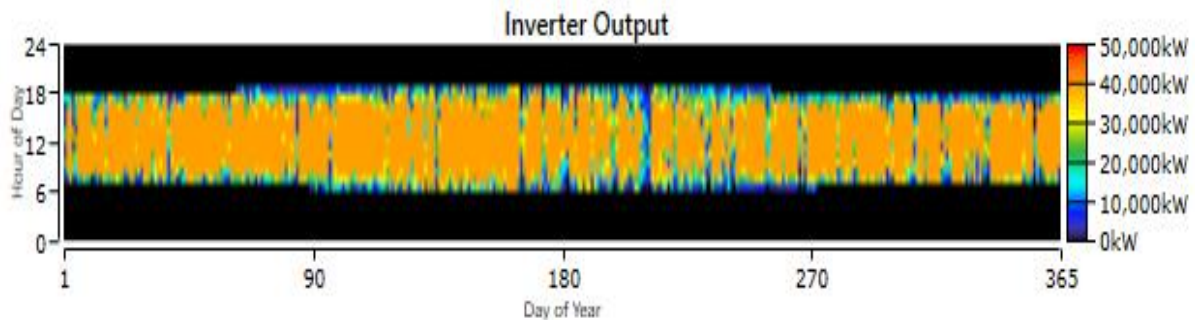


Figure 18: optimal design inverter output

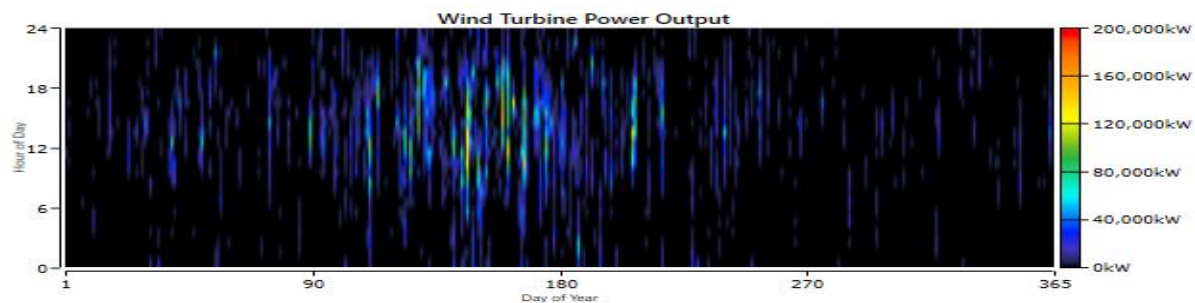


Figure 19: Optimal case- wind turbine output

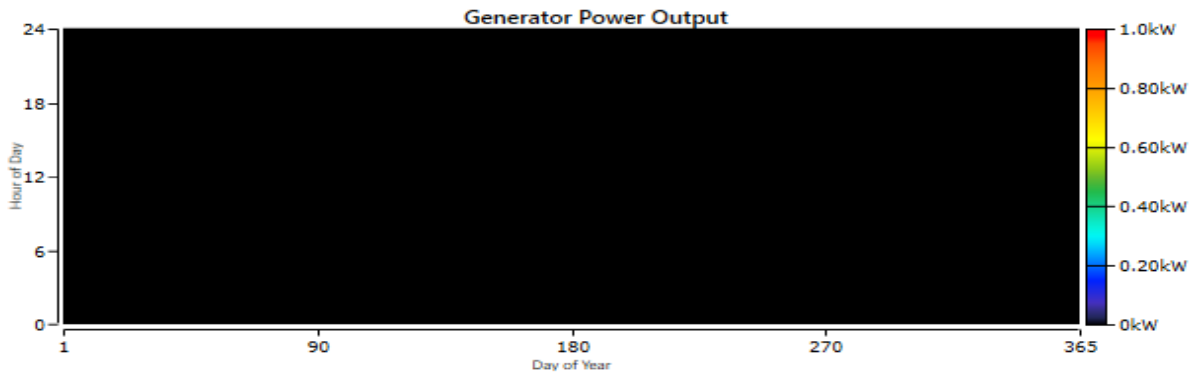


Figure 20: Optimal case- diesel generator power output

The solar PV system's power output is depicted in Figure 17 throughout the day. The PV system generates between 40,000 and 120,000 kW during the day, which is represented by the dark-pink colour on the graph. At night, the PV power output decreases to zero, which is represented by the black colour. Figure 18 shows the inverter output, which is a mirror image of the PV power output. Since the inverter only functions when the PV system generates power—that is, when it converts the DC power produced by the PV system into AC power for the load—it is high during the day when the PV generation is active and zero at night.

The power output of wind turbines is shown in Figure 19, and it varies both daily and annually. Dispersed blue colours on the graph represent different wind outputs between 0 and 30,000 kW. The periods of 0% wind power output are indicated by the dark areas. This fluctuation in wind speed emphasizes how sporadic wind energy is, in contrast to solar PV generation's more consistent daily rhythm. Figure 20 depicts generation from a diesel generator, as shown in the figure 20, do generation comes from the diesel engine as its only used as a backup. Together, these Figures highlight how much of the daytime energy generation is dependent on solar PV and how important the inverter is in transforming that energy into usable form. In the meantime, the wind turbine supplements the solar PV output with additional, albeit erratic, power. This emphasizes the necessity of grid support to keep an even energy supply, particularly when there are no solar periods.

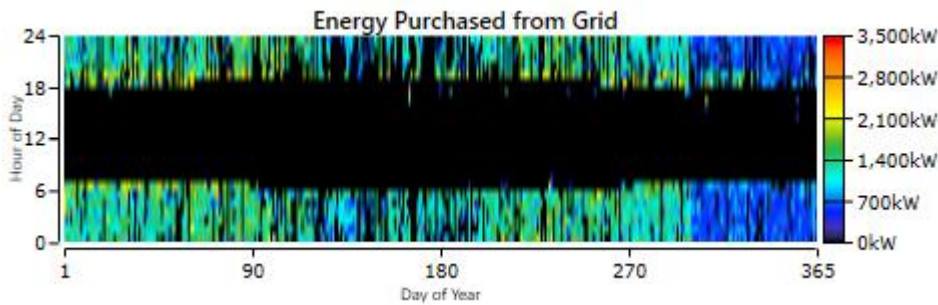


Figure 21: Optimal design energy purchase from the grid

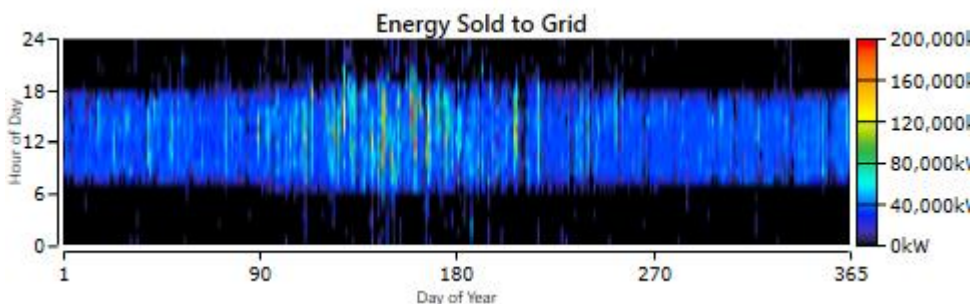


Figure 22: Optimal design energy sold to the grid

The proposed design's grid-purchased energy pattern is depicted in Figure 21. The line is black from 6 a.m. to 6 p.m., which indicates almost no energy purchases from the grid. This time frame corresponds with the sun and wind availability, which supply enough energy for production. Not only is the energy demand satisfied during these hours, but excess energy is also produced and sold back to the system. However, because solar energy is unavailable between 6 p.m. and 6 a.m., the scenario shifts. The blue areas on the graph indicate purchases ranging from 0 to 700 kW, which correspond to the portion of the energy demand that is met during these overnight hours by importing energy from the grid. The energy sold to the grid is displayed in Figure 22. Excess energy is produced during the day and sold to the grid; sales of 10,000 to 40,000 kW are represented by the blue hue on the graph. In contrast, during the night, when wind and solar PV production fluctuate and production from PV stops, the graph turns black, signifying that no energy is sold to the grid. The idea behind this system is net metering, in which excess energy generated during the day is fed into the grid and energy is bought from it at night when the amount of renewable energy produced is at its lowest. By making up for the extra energy produced during the day, the grid ensures a steady supply of electricity to fulfil demand while also yielding financial benefits. By utilizing solar and wind energy during the day and depending on the grid for support at night, this system efficiently balances the production and consumption of energy.

3.3. Technical superiority of the proposed system

The base case, which only uses wind turbines and the grid, is greatly outperformed by the suggested solution, which combines solar PV, wind turbines, a diesel generator, and grid connectivity. The base case's 67,056,840 kWh/year is about five times less than the 325,773,288 kWh/year produced by the proposed system. Using net metering to generate revenue, excess energy generated during the day is sold to the grid for 167,761,193 kWh annually, while 3,827,194 kWh are purchased at night. This system is both technically and financially better than the base case since it not only provides a consistent supply of energy from a variety of sources but also makes a sizable profit from grid sales.

3.4. Economic analysis of the proposed system

When compared to the base case, which only uses wind turbines and the grid, the proposed energy system—which combines solar PV, wind turbines, a diesel generator, and grid support—significantly improves economic feasibility. Tables 7 and 11 illustrate that the base case's total start-up and replacement costs come to \$13,523,393, while the proposed system's total comes to \$16,207,384. Nonetheless, the significant financial advantages that the suggested strategy offers outweigh these additional expenses. The proposed system's Return on Investment (ROI) is 10.1% as shown in Table 12, a significant increase from the base case's meager 0.54% as depicted in Table 8. This suggests that, in comparison to the capital invested, the proposed approach generates far higher financial returns. The proposed system's Levelized Cost of Energy (LCOE), which is \$0.00146/kWh as opposed to \$0.0413/kWh for the base case, is likewise much lower. The proposed system is significantly more cost-effective in terms of energy generation over the course of its operating lifespan, as evidenced by its reduced LCOE. Operational and Maintenance (O&M) costs are comparable between the two systems, with the proposed system having slightly higher O&M costs (\$3,518,963) due to the additional components as Tables 7 and 12 depict. However, these costs are offset by the increased reliability and higher energy production capacity. The proposed system's diversified energy sources—solar PV, wind, and a diesel generator—ensure a more reliable and consistent energy supply, reducing the reliance on grid purchases and enhancing overall system performance. In terms of economics, the proposed energy system is better than the base case, its considerably better ROI, lower LCOE, higher current value, and significantly higher yearly worth more than offset its higher original expenditure.

3.5. Sensitivity analysis of the proposed design

Table 13: Technical results of sensitivity analysis of the proposed designed

| Sensitivity | Solar irradiance (kWh/m ² /day) | Wind speed (m/s ²) | Fuel price (\$/Litre) | Energy production (kWh/yr) |
|-------------|--|--------------------------------|-----------------------|----------------------------|
| 80% | 4.10 | 2.94 | 1.08 | 183,464,902 |
| 100% | 5.12 | 3.67 | 1.08 | 305,773,288 |
| 120% | 6.14 | 4.40 | 1.08 | 400,563,007 |
| 140% | 7.17 | 5.14 | 1.08 | 487,179,527 |
| 150% | 7.68 | 5.51 | 1.08 | 528,914,590 |

Table 14: Economic results of sensitivity analysis of the proposed designed

| Sensitivity of energy production (kWh/yr) | Grid price (\$/kWh) | LCOE (\$/kWh) | NPC (\$) | O & M cost (\$) |
|---|---------------------|---------------|------------|-----------------|
| 80% | 0.1 | 0.00723 | 11,965,907 | 3,167,024 |
| 100% | 0.1 | 0.00146 | 16,207,384 | 3,518,963 |
| 120% | 0.092 | 0.00101 | 18,348,760 | 3,760,859 |
| 140% | 0.089 | 0.00087 | 20,689,022 | 3,922,755 |
| 150% | 0.088 | 0.00077 | 23,245,780 | 4,001,651 |

The robustness and adaptability of the proposed energy system—which includes solar PV, wind turbines, a diesel generator, and grid support—under various situations are demonstrated by the sensitivity analysis of the system. Technically, variations in wind speed and sun irradiation cause a considerable variation in the amount of energy produced. The system generates 183,464,902 kWh annually at 80% of standard circumstances, which are 4.10 kWh/m²/day for solar irradiation and 2.94 m/s² for wind speed. Production is 305,773,288 kWh/year at 100% standard conditions; at 150% conditions, it increases significantly to 528,914,590 kWh/year (7.68 kWh/m²/day for solar irradiation and 5.51 m/s² for wind speed) as presented in Table 13. This suggests that the system's output is very sensitive to changes in the availability of solar and wind energy, producing considerable increases in energy output as resource availability rises. The study demonstrates that, in terms of economics, the various production scenarios exhibit positive Net Present Costs (NPC) and Levelized Costs of Energy (LCOE) as presented in Table 14. The LCOE is \$0.00723/kWh at 80% energy output, with an NPC of \$11,965,907 and O&M expenses of \$3,167,024. When production reaches 100%, the LCOE decreases to \$0.00146/kWh, the NPC is \$16,207,384, and O&M expenses come to \$3,518,963. The LCOE drops to \$0.00077/kWh as output reaches 150%, the NPC increases to \$23,245,780, and O&M expenses total \$4,001,651. This shows that by taking advantage of economies of scale, the suggested system becomes more economically efficient as energy production rises.

The proposed design is substantially less susceptible to changes in fuel prices, grid prices, and the availability of renewable resources than the base case. Incorporating solar photovoltaics and a diesel generator results in a more consistent and varied energy output, decreasing dependency on grid power and lessening the effects of price increases. The suggested system is a better option than the base case, which only uses wind turbines and grid assistance, since it has a lower lifetime cost of ownership and a higher net present value (NPC) across a range of scenarios. The technical and financial feasibility of the suggested system is confirmed by this thorough sensitivity study for a variety of operational scenarios

4. Conclusion

In conclusion the proposed microgrid design, incorporating PV solar panels, wind turbines, and grid integration, is a highly effective solution for addressing the energy challenges faced by Mewar University. The optimized system significantly reduces energy costs and dependency on diesel generators and the grid, resulting in substantial environmental benefits through decreased greenhouse gas emissions. The microgrid design achieves an impressively low levelized cost of energy (LCOE) of

\$0.00146/kWh and a favourable return on investment (ROI) of 10.1%, demonstrating its economic viability. With 83% of the annual energy production sourced from solar photovoltaics and 17% from wind turbines and the grid, the system ensures a reliable and sustainable energy supply. Comprehensive feasibility, technical, economic, and sensitivity analyses confirm the practicality and effectiveness of the proposed microgrid, making it a promising energy solution for the university's future needs.

References

- [1] Battula, A., Vuddanti, S., & Salkuti, S. (2021). Review of Energy Management System Approaches in Microgrids. *Energies*. <https://doi.org/10.3390/en14175459>.
- [2] Guo, Y., & Zhao, C. (2018). Islanding-Aware Robust Energy Management for Microgrids. *IEEE Transactions on Smart Grid*, 9, 1301-1309. <https://doi.org/10.1109/TSG.2016.2585092>.
- [3] Wang, B., Dabbaghjamanesh, M., Kavousi-fard, A., & Mehraeen, S. (2019). Cybersecurity Enhancement of Power Trading Within the Networked Microgrids Based on Blockchain and Directed Acyclic Graph Approach. *IEEE Transactions on Industry Applications*, 55, 7300-7309. <https://doi.org/10.1109/TIA.2019.2919820>.
- [4] Badal, F., Sarker, S., Nayem, Z., Moyeen, S., & Das, S. (2022). Microgrid to smart grid's evolution: Technical challenges, current solutions, and future scopes. *Energy Science & Engineering*, 11, 874 - 928. <https://doi.org/10.1002/ese3.1319>.
- [5] Hu X, Martinez CM, Yang Y (2016) Charging, power management, and battery degradation mitigation in plug-in hybrid electric vehicles: a unified cost-optimal approach. *Mech Syst Signal Process* 87: 4–16. <https://doi.org/10.1016/j.ymssp.2016.03.004>
- [6] Hu X, Moura SJ, Murgovski N, Egardt B, Cao D (2016) Integrated optimization of battery sizing, charging, and power management in plug-in hybrid electric vehicles. *IEEE Trans Control Syst Technol* 24(3):1036–1043
- [7] Demirbas A (2016) Future energy sources. *Waste energy for life cycle assess*. Springer Inter Pub:33–70
- [8] Kumar P, Palwalia DK (2015) Decentralized autonomous hybrid renewable power generation. *J of Renew Energy (Hindawi Pub Corp)*:1–18
- [9] Akikur RK, Saidur R, Ping HW, Ullah KR (2013) Comparative study of stand-alone and hybrid solar energy systems suitable for off-grid rural electrification: a review. *Renew Sust Energy Rev* 27: 738–752
- [10] Bhandari B, Poudel SR, Lee KT, Ahn SH (2014) Mathematical modeling of hybrid renewable energy system: a review on small hydro-solar-wind power generation. *Int J of Precision Engg and Manufac-Green Tech* 1(2):157–173
- [11] Chauhan RK, Rajpurohit BS, Singh SN, Gonzalez-Longatt FM (2014) DC grid interconnection for conversion losses and cost optimization. *Renew energy integration: challenges and solutions*. Springer Singapore:327–345
- [12] Chauhan RK, Rajpurohit BS, Gonzalez-Longatt FM, Singh SN (2016) Intelligent energy management system for PV-battery-based micro-grids in future dc homes. *Int J Emerg Electr Power Syst* 17. <https://doi.org/10.1515/ijeeps-2015-0210>
- [13] Kumar YVP, Ravikumar B (2016) Integrating renewable energy sources to an urban building in India: challenges, opportunities, and techno-economic feasibility simulation. *Tech and Economics of Smart Grids and Sust Energy* 1(1):1–16
- [14] Shezan SA, Julai S, Kibria MA, Ullah KR, Saidur R, Chong WT, Akikur RK (2016) Performance analysis of an off-grid wind-PV (photovoltaic)-diesel-battery hybrid energy system feasible for remote areas. *J Clean Prod* 125:121–132
- [15] Lal S, Raturi A (2012) Techno-economic analysis of a hybrid mini-grid system for Fiji islands. *Int J of Energy and Env Engg* 3(1):1–10
- [16] Kazem HA, Al-Badi HA, Al Busaidi AS, Chaichan MT (2016) Optimum design and evaluation of hybrid solar/wind/diesel power system for Masirah Island. *Environ Dev Sustain* 19:1–18. <https://doi.org/10.1007/s10668-016-9828-1>

- [17] El-Madany HT, Fahmy FH, El-Rahman NMA, Dorrah HT (2012) Design of FPGA based neural network controller for earth station power system. *Telkomnika Telecom, Compu, Electro and Cont* 10(2):281–290
- [18] Kusakana K, Vermaak HJ (2013) Hybrid renewable power systems for mobile telephony base stations in developing countries. *Renew Energy* 51:419–425
- [19] Shezan SA, Saidur R, Ullah KR, Hossain A, Chong WT, Julai S (2015) Feasibility analysis of a hybrid off-grid wind–DG–battery energy system for the eco-tourism remote areas. *Clean Tech Environ Policy* 17(8):2417–2430
- [20] Afonso C, Rocha C (2016) Evaluation of the economic viability of the application of a trigeneration system in a small hotel. *Future Cities and Envir* 2(1):1–9
- [21] Yang HX, Zhou W, Lou CZ (2009) Optimal design and techno-economic analysis of a hybrid solar–wind power generation system. *Appl Energy* 86:163–169
- [22] Chauhan RK, Rajpurohit BS, Hebner RE, Singh SN, Gonzalez-Longatt FM (2016) Voltage standardization of dc distribution system for residential buildings. *J of Clean Energy Tech* 4(3):167–172
- [23] Speidel S, Bräunl T (2016) Leaving the grid—the effect of combining home energy storage with renewable energy generation. *Renew Sust Energ Rev* 60:1213–1224
- [24] Zou Y, Hu X, Ma H, Li SE (2015) Combined state of charge and state of health estimation over lithium-ion battery cell cycle lifespan for electric vehicles. *J Power Sources* 273:793–803
- [25] Hu X, Jiang J, Cao D, Egardt B (2016) Battery health prognosis for electric vehicles using sample entropy and sparse Bayesian predictive modeling. *IEEE Trans Ind Electron* 63(4):2645–2656
- [26] Khare V, Nema S, Baredar P (2016) Solar–wind hybrid renewable energy system: a review. *Renew Sust Energ Rev* 58:23–33
- [27] Zhou W, Lou C, Li Z, Lu L, Yang H (2010) Current status of research on optimum sizing of stand-alone hybrid solar–wind power generation systems. *Appl Ener* 87(2):380–389
- [28] Beal CD, Gurung TR, Stewart RA (2016) Modelling the impacts of water efficient technologies on energy intensive water systems in remote and isolated communities. *Clean Techn Environ Policy* 18(6):1713–1723
- [29] Ranaweera I, Kolhe ML, Gunawardana B (2016) Hybrid energy system for rural electrification in Sri Lanka: design study. *Solar Photo Sys Appl*, Springer International Publishing:165–184
- [30] Ma T, Yang H, Lu L (2014) A feasibility study of a stand-alone hybrid solar–wind–battery system for a remote island. *Appl Energy* 121:149–158
- [31] Khalilpour KR, Vassallo A (2016) Economic analysis of leaving the grid. *Commu energy net with storage*. Springer Singapore:105–130
- [32] Olatomiwa L, Mekhilef HASN, Ohunakin OS (2015) Economic evaluation of hybrid energy systems for rural electrification in six geo-political zones of Nigeria. *Renew Energy* 83:435–446
- [33] Reddy SS, Panigrahi BK, Kundu R, Mukherjee R, Debchoudhury S (2013) Energy and spinning reserve scheduling for a wind-thermal power system using CMA-ES with mean learning technique. *Elect Power Energy Syst* 53:113–122
- [34] Ghaffari R, Venkatesh B (2013) Options based reserve procurement strategy for wind generators—using binomial trees. *IEEE Trans Power Syst* 28(2):1063–1072
- [35] Delucchi MA, Jacobson MZ (2011) Providing all global energy with wind, water, and solar power, part II: reliability, system and transmission costs, and policies. *Energy Policy* 39:1170–1190
- [36] Khatir AA, Cherkaoui R (2011) A probabilistic spinning reserve market model considering DisCo' different value of lost loads. *Elect Power Syst Res* 81:862–872
- [37] Jones BW, Powell R (2015) Evaluation of distributed building thermal energy storage in conjunction with wind and solar electric power generation. *Renew Energy* 74:699–707

- [38] Parastegari M, Hooshmand RA, Khodabakhshian A, Zare AH (2015) Joint operation of wind farm, photovoltaic, pump-storage and energy storage devices in energy and reserve markets. *Elect Power Energy Syst* 64:275–284
- [39] Wua K, Zhou H, An S, Huang T (2015) Optimal coordinate operation control for wind–photovoltaic–battery storage power-generation units. *Energy Convers Manag* 90:466–475
- [40] Kumaravel S, Ashok S (2015) Optimal power management controller for a stand-alone solar PV/wind/battery hybrid energy system. *Energy Sources* 37(4):407–415
- [41] Singh SN, Gonzalez-Longatt FM (2014) Operation and control of HVDC grids for renewable energy integration: state-of-the-art and future trends. *Renew Energy Integration: Challenges and Solutions*. Springer: 227-244
- [42] Chauhan RK, Rajpurohit BS (2015) Techno-economic analysis of hybrid renewable energy system for rural electrification in India. *International Journal of Electrical Power & Energy Systems* 74: 150-157
- [43] A. S. Aziz, M. F. N. Tajuddin, M. R. Adzman, M. F. Mohammed, and M. A. M. Ramli, "Feasibility analysis of grid-connected and islanded operation of a solar PV microgrid system: A case study of Iraq," *Energy*, vol. 191, Jan. 2020, Art. no. 116591.
- [44] S. Singh, P. Chauhan, and N. Singh, "Capacity optimization of grid connected solar/fuel cell energy system using hybrid ABC-PSO algorithm," *Int. J. Hydrogen Energy*, vol. 45, no. 16, pp. 10070–10088, Mar. 2020.
- [45] H. Taghavifar and Z. S. Zomorodian, "Techno-economic viability of on grid micro-hybrid PV/wind/Gen system for an educational building in Iran," *Renew. Sustain. Energy Rev.*, vol. 143, Jun. 2021, Art. no. 110877.
- [46] C. A. Nallolla, "Optimal design of a hybrid off-grid renewable energy system using techno-economic and sensitivity analysis for a rural remote location," *Sustainability*, vol. 14, no. 22, p. 15393, Nov. 2022.
- [47] D. M. Mahmud, S. M. M. Ahmed, S. Hasan, and M. Zeyad, "Grid-connected microgrid: Design and feasibility analysis for a local community in Bangladesh," *Clean Energy*, vol. 6, no. 3, pp. 447–459, Jun. 2022.
- [48] A. Maleki, M. G. Khajeh, and M. A. Rosen, "Two heuristic approaches for the optimization of grid-connected hybrid solar–hydrogen systems to supply residential thermal and electrical loads," *Sustain. Cities Soc.*, vol. 34, pp. 278–292, Oct. 2017.
- [49] H. Ren, Q. Wu, W. Gao, and W. Zhou, "Optimal operation of a grid-connected hybrid PV/fuel cell/battery energy system for residential applications," *Energy*, vol. 113, pp. 702–712, Oct. 2016.
- [50] Alshehri, M., Guo, Y., & Lei, G. (2023). Renewable-Energy-Based Microgrid Design and Feasibility Analysis for King Saud University Campus, Riyadh. *Sustainability*. <https://doi.org/10.3390/su151310708>
- [51] Zhou, Y., Panteli, M., Moreno, R., & Mancarella, P. (2018). System-level assessment of reliability and resilience provision from microgrids. *Applied Energy*. <https://doi.org/10.1016/J.APENERGY.2018.08.054>.
- [52] Garmabdari, R. (2020). Multi-Energy Microgrid Systems Planning and Energy Management Optimisation. . <https://doi.org/10.25904/1912/4001>.
- [53] Tasnim, S., Hosseizadeh, N., Mahmud, A., & Gargoom, A. (2020). How VPPs Facilitate the Integration of Renewable Energy Sources in the Power Grid and Enhance Dispatchability - A Review. 2020 Australasian Universities Power Engineering Conference (AUPEC), 1-6.
- [54] Zia, M., Elbouchikhi, E., & Benbouzid, M. (2018). Microgrids energy management systems: A critical review on methods, solutions, and prospects. *Applied Energy*. <https://doi.org/10.1016/J.APENERGY.2018.04.103>.
- [55] Zone, S. S. E. (2012). Rajasthan Solar Park–An Initiative Towards Empowering Nation.
- [56] P. K. Sahu, S. Jena, and U. Sahoo, "Techno-economic analysis of hybrid renewable energy system with energy storage for rural electrification," *Hybrid Renew. Energy Syst.*, vol. 12, pp. 63–96, Feb. 2021, doi: 10.1002/9781119555667.ch3.
- [57] T. Adefarati and G. D. Obikoya, "Techno-economic evaluation of a grid-connected microgrid system," *Int. J. Green Energy*, vol. 16, no. 15, pp. 1497–1517, Dec. 2019.

- [58] Alluraiah, N. C., & Vijayapriya, P. (2023). Optimization, design and feasibility analysis of a grid-integrated hybrid AC/DC microgrid system for rural electrification. *Ieee Access*.
- [59] O. Krishan and S. Suhag, "Techno-economic analysis of a hybrid renewable energy system for an energy poor rural community," *J. Energy Storage*, vol. 23, pp. 305–319, Jun. 2019.
- [60] National Renewable Energy Laboratory. Accessed: Jun. 24, 2022. [Online]. Available: <http://www.nrel.gov>
- [61] Discover Innovative Battery Solutions. Accessed: Jul. 16, 2022. [Online]. Available: <http://surl.li/gorcn>
- [62] H. K. Pujari and M. Rudramoorthy, "Optimal design, prefeasibility technoeconomic and sensitivity analysis of off-grid hybrid renewable energy system," *Int. J. Sustain. Energy*, vol. 12, no. 1, pp. 1–33, 2022, doi: 10.1080/14786451.2022.2058502.
- [63] Tay, G., Acakpovi, A., Adjei, P., Aggrey, G. K., Sowah, R., Kofi, D., ... & Sulley, M. (2022, July). Optimal sizing and techno-economic analysis of a hybrid solar PV/wind/diesel generator system. In *IOP Conference Series: Earth and Environmental Science* (Vol. 1042, No. 1, p. 012014). IOP Publishing.
- [64] Deevela N R, Singh B and Kandpal T C 2018 Load Profile of Telecom Towers and Potential Renewable Energy Power Supply Configurations Proceedings of 2018 IEEE International Conference on Power Electronics, Drives and Energy Systems, PEDES 2018
- [65] Salisu S, Mustafa M W, Olatomiwa L and Mohammed O O 2019 Assessment of technical and economic feasibility for a hybrid PV-wind-diesel-battery energy system in a remote community of north central Nigeria Alexandria Engineering Journal 58 1103–18
- [66] Essalaimeh S, Al-Salaymeh A and Abdullat Y 2013 Electrical production for domestic and industrial applications using hybrid PV-wind system Energy Conversion and Management 65
- [67] Kabalci E 2013 Design and analysis of a hybrid renewable energy plant with solar and wind power Energy Conversion and Management 72
- [68] Li C, Ge X, Zheng Y, Xu C, Ren Y, Song C and Yang C 2013 Techno-economic feasibility study of autonomous hybrid wind/PV/battery power system for a household in Urumqi, China Energy 55
- [69] El Badawe M, Iqbal T and Mann G K 2012 Optimization and a comparison between renewable and non-renewable energy systems for a telecommunication site 2012 25th IEEE Canadian Conference on Electrical and Computer Engineering: Vision for a Greener Future, CCECE 2012
- [70] Ghoddami H, Delghavi M B and Yazdani A 2012 An integrated wind-photovoltaic-battery system with reduced power-electronic interface and fast control for grid-tied and off-grid applications Renewable Energy 45
- [71] Daud A K and Ismail M S 2012 Design of isolated hybrid systems minimizing costs and pollutant emissions Renewable Energy 44